J. Indian Chem. Soc.,
Vol. 97, No. 11a, November 2020, pp. 2180-2187

Effect of substrate and substrate temperature on microstructure of magnetron sputtering doped-ZnO thin films

Himadri Sekhar Das*[a,b], Rajesh Das[b], Gourisankar Roymahapatra[b] and Prasanta Kumar Nandi[a]

[a]Department of Chemistry, Indian Institute of Engineering Science and Technology (IIEST), Shibpur, Howrah-711 103, West Bengal, India

[b]School of Applied Science and Humanities, Haldia Institute of Technology, Haldia-721 657, West Bengal, India

E-mail: himadrisekhar_das@rediffmail.com

Manuscript received online 01 October 2020, revised and accepted 31 October 2020

Al and Ga doped ZnO thin films were deposited on glass, polyethylene naphthalate (PEN) and Si substrate with variation of substrate temperature (Ts) by RF magnetron sputtering. X-Ray diffraction patterns of ZnO:Al (AZO) and ZnO:Ga (GZO) film shows strong peak (002) with a hexagonal wurtzite structure preferentially oriented along the C-axis and have a good crystallinity on Si (100) substrate. But it is observed that the peak position is shifted from its mean position for both; high and room temperature deposited films. Intrinsic stress is developed between substrate molecule and ZnO thin films and as a result; structural defects, voids, and micro-crack are observed for AZO thin film deposited at substrate temperature 400°C due to variation of internal texture. Film strain significantly affects on its mechanical properties, cohesion properties, and electrical conductivity. Electrical resistivity came 4.9×10^{-4} Ω-cm and 4.5×10^{-4} Ω-cm for AZO and GZO respectively on glass substrate with optical transmission more than 90%. AZO on PEN (polyethylene terephthalate) substrate shows the resistivity of 8.6×10^{-4} Ω-cm at room temperature.

Keywords: ZnO:Al, ZnO:Ga, polyethylene terephthalate (PEN), RF magnetron sputtering, flexible display.

Introduction

In recent time, transparent conducting oxide (TCO) films is a major interesting research subject, due to its wide use in optoelectronic devices such as low-emissivity windows, electromagnetic shielding, gas sensors, information displays, and photovoltaic cells. SnO_2 and ITO (Indium tin oxide) are the commercially available transparent conductive oxide thin films[1,2] at present, but indium is a rare metal with high toxicity. Doped ZnO thin film is considered to be the most promising material as TCO thin films for its high optical transmittance (> 90%) and very low electrical resistivity (in the order of 10^{-5} Ω-cm). ZnO thin film can be deposited in either physical or chemical vapor deposition techniques such as; sol-gel method, spray pyrolysis, pusled laser deposition, thermal evaporation, molecular beam Epitaxy and RF magnetron sputtering[3–6]. RF magnetron sputtering technique is mostly preferred due to its reproducibility, high orientation and uniformity in films. Non-toxicity, high crystallinity and stability against hydrogen plasma; makes the doped ZnO films commercially more viable with respect to ITO and SnO_2[7,8]. This advantages makes ZnO:Al suitable for flexible display, solar cell and other photovoltaic applications[9,10]. Nowadays researchers are working to improve the flat panel display technology by replacing glass substrate with flexible polymer[11].

The growth of thin film such as; lattice growth, thermal mismatching between thin layer and the substrate, depend on the substrate types. Nucleation and binding of thin layer also depends on the movement of the substrate. The properties of the deposited thin films vary for different deposition techniques. Stress can change the electrical and optical properties of the grown thin films. The stress comes due to the formation of defects or due to extrinsic doping.

Deniz *et al.* prepared the undoped ZnO and ZnO:Al thin films with different Al concentrations onto Si(100) substrate by PFCVAD (Pulsed Filtered Cathodic Vacuum Arc Deposition) technique at room temperature, and investigated the

influence of doping on the structural and optical properties of thin films[12]. They achieved the highest reflectance values of about 35% in the wavelength range of 400–800 nm. Mohit *et al*. systematically investigated the dependence of RF power on the physical properties of AZO thin films on PEN substrate[13]. Xiaojin *et al.* studied the effect of substrate on electrical and optical properties of AZO thin film deposited by RF magnetron sputtering. In their study they achieved the lowest resistivity of 12.52×10^{-4} Ω-cm and low visible transmission of 85% on glass substrate respectively[14]. Bassam *et al.* studied the effect of O_2 on structural and optical properties of ZnO thin film deposited on glass and Si(100) substrate by RF magnetron sputtering technique[15]. They reported the different properties such as optical, electrical and surface morphology of the thin films, but they didn't study the effect of haze factor. In 2016, Hamrit *et al.* studied the RF magnetron sputtered ZnO:Al thin film (500 nm thickness) on PEN substrate. They reported the electrical resistance 4×10^{-4} Ω-cm with 80% optical transmission[16]. Ghosh *et al.* studied the effect of substrate induced strain in poly crystalline ZnO thin films on different substrate[17]. Rajesh *et al.* reported the effect of intrinsic stress on the optical properties of ZnO films[18]. Doped ZnO thin film grown on bulk Si substrate is an interesting subject for application as a photon window for photodiode, and wafer-based silicon solar cell[19].

In this paper, effect of different substrates (glass, Si and PEN) and substrate temperature have been studied on ZnO:Al and ZnO:Ga thin films. Substrate dependent electrical, optical, micro-structural and Haze properties at different substrate temperature (T_s, °C) have been investigated.

Experimental

ZnO:Al and ZnO:Ga thin films were deposited on glass, Si and PEN substrate at different T_s by dual-target RF (13.56 MHz frequency) magnetron sputtering technique (Hind High Vacuum Co. (P.) Ltd.) under non reactive environment (Ar ambient) using 99.99% pure sintered ceramic disc with sputtering targets (2 inch in diameter and 5 mm in thickness) of ZnO:Al (2 wt% Al) and ZnO:Ga (3 wt% Ga) respectively.

Ar flow was maintained at 40 sccm throughout the experiment. All the films are deposited on different substrate on different substrate temperature with RF power 100 watt with of 5.6×10^{-6} mbar base pressure. To achieve the uniform growth of doped (Al, Ga) ZnO thin films with high deposition rate and good adhesion to the substrate material, the target was located at top of the chamber and the substrate at the bottom. The surface oxide layer of the target (impurity) and the glass substrate were cleaned by plasma cleaning method before thin film deposition. For that, pre-sputtering in pure argon plasma atmosphere was carried out for 15 min. Uniform distance between substrate to target (about 6 cm) was maintained throughout the experiment.

The electrical properties (resistivity, carrier concentration and Hall mobility) of doped (Al, Ga) ZnO thin films were studied by 4-probe van-der-Pauw technique attached with Hall measurement set-up (Ecopia-HMS-3000). Optical transmittance (transmittance, reflectance and Haze) of thin films was measured using double beam UV-Vis (Perkin-Elmer Lamda-35) spectrophotometer. The structural characterization of doped (Al, Ga) ZnO thin films were carried out by XRD technique (Philips PW 1710 diffractometer, Cu Kα radiation, λ = 1.54178 Å, 2θ scan mode). Surface topography of doped (Al, Ga) ZnO films were studied by Atomic Force Microscopy (AFM) (Multimode 8, Bruker).

Results and discussion

Doped ZnO thin films were deposited with 100 W RF power, 10 mbar chamber pressure, different substrate temperature with controlled substrate rotation under non-reactive environment (Ar atmosphere). AZO and GZO thin films show promising electrical properties [$\rho = 4.9\times10^{-4}$ Ω-cm (Al) and 4.5×10^{-4} Ω-cm (Ga)] due to its high carrier density and nearly 90% optical transmission. Those properties are comparable with sputtered ITO and U-type SnO_2:F thin films (R_{sh}< 5 Ω/sq.) due to both high carrier density ($\times10^{20}$/cm^3) and mobility. Temperature dependent electrical resistivity, carrier concentration and mobility of as-deposited ZnO:Al and ZnO:Ga thin films on different substrate are (up to substrate temperature T_s = 400°C) listed in Table 1. It was observed that resistivity decreases as the deposition temperature increases up to 300°C for both ZnO:Ga and ZnO:Al, but above 300°C the resistivity increases due to increases of free carrier scattering, grain boundary scattering and for lowering of mobility.

The electrical properties of doped ZnO thin films were investigated at room temperature. To apply the thin film in

Table 1. Variation of electrical parameter with different T_s of doped (Al, Ga) ZnO thin films

Substrate type	Substrate temperature T_s (°C)	Resistivity (Ω -cm)	Mobility (cm^2/V.s)	Carrier concentration (/cm^3)	Figure of merit (FOM)
ZnO:Al/Glass	27	8.6×10^{-3}	3.6	4.5×10^{20}	2.30×10^{18}
	200	6.3×10^{-4}	8.0	9.3×10^{20}	1.16×10^{18}
	300	4.9×10^{-4}	11.0	7.1×10^{20}	1.08×10^{18}
	400	5.7×10^{-3}	2.3	4.3×10^{20}	2.01×10^{18}
ZnO:Ga/Glass	27	6.5×10^{-4}	8.0	9.4×10^{20}	1.20×10^{17}
	200	5.9×10^{-4}	8.2	9.6×10^{20}	1.70×10^{17}
	300	4.5×10^{-4}	10.0	1.3×10^{21}	5.90×10^{17}
	400	5.4×10^{-3}	2.6	3.9×10^{20}	1.60×10^{17}
ZnO:Al/PEN	27	8.6×10^{-4}	5.2	1.4×10^{21}	1.14×10^{18}

Solar cell as front/back reflector and flexible display, the substrate temperature were also kept at room temperature.

Fig. 1 shows the optical transmittance spectra of AZO and GZO thin films on glass and PEN substrate with a high optical transmission of 90% and 85% respectively in the visible range of the solar spectrum. The ZnO:Ga thin film on glass substrate shows the transmission more than 90% in the visible region. Effect of substrate on transmission and reflectance were shown on Fig. 1 and Fig. 2 respectively. The transmittance spectra show a sharp absorption edge at 330–400 nm range. Reflectance spectra of AZO show the characteristic nature of thin film in different substrates.

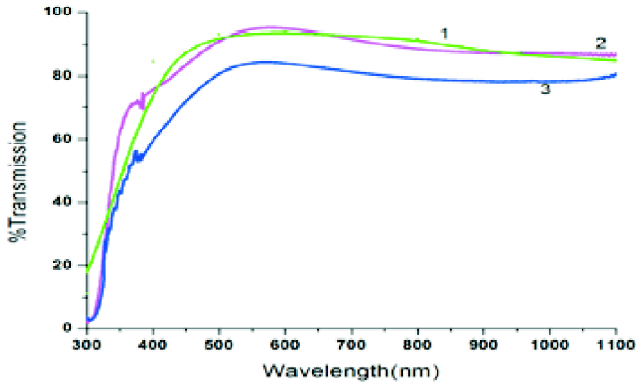

Fig. 1. Transmission spectra of (1) ZnO:Al (green), (2) ZnO:Ga film on glass (pink) and (3) ZnO:Al on PEN substrate (blue).

Fig. 3 shows the photoluminescence spectra of ZnO:Al thin film on glass and PEN substrates within the range 360–500 nm. Films shows the excitonic peak in the UV region (370–385 nm), and no visible emission spectra was observed,

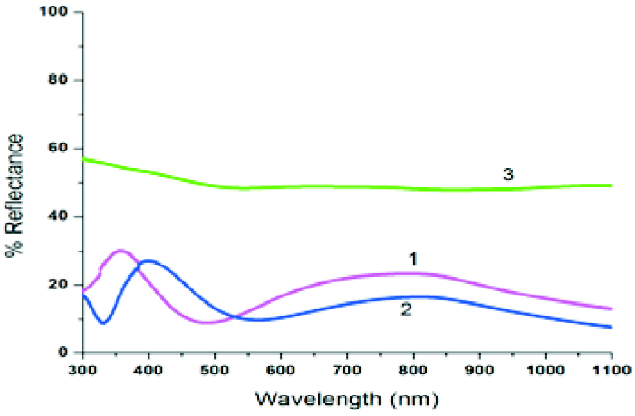

Fig. 2. Reflectance spectra of ZnO:Al film on different substrate: (1) glass (pink), (2) PEN (blue) and (3) Si (green).

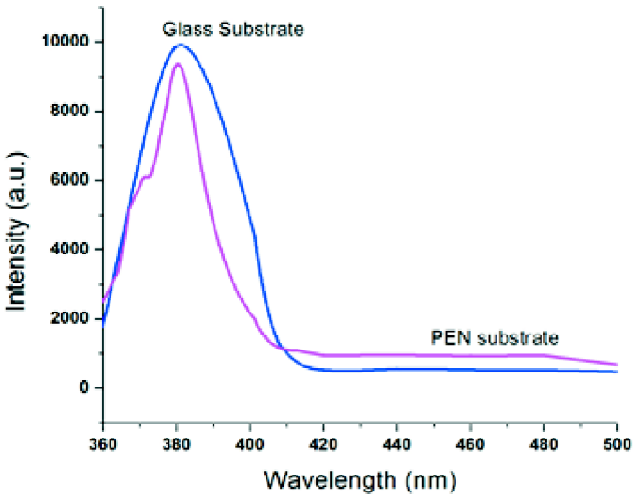

Fig. 3. Photoluminescence spectra of ZnO:Al film on different substrate.

that's mean deposited films have a good optical quality.

The structural parameters were investigated from X-ray diffraction (XRD) analysis. XRD footprint of doped ZnO thin films on PEN (at RT) and on glass substrate (at different T_s = 200°C, 300°C, 400°C) are shown in Fig. 4 and Fig. 5 respectively, and Fig. 6 shows the XRD pattern of ZnO:Al thin film on Si substrate. In all XRD spectra for the ZnO:Al thin films, the appearance of films intensity of (002) peaks indicate that, the film is preferentially c-axis oriented.

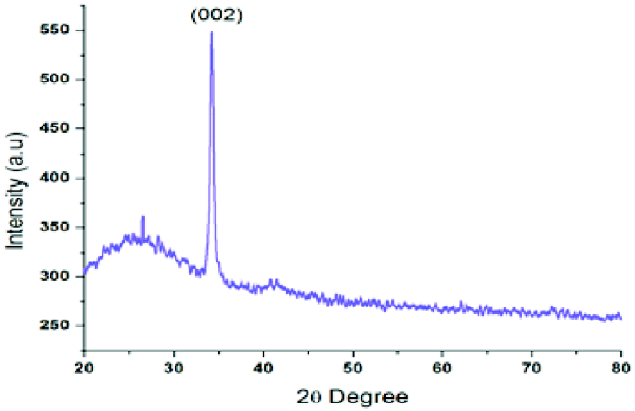

Fig. 4. XRD pattern of ZnO:Al film on PEN substrate at RT.

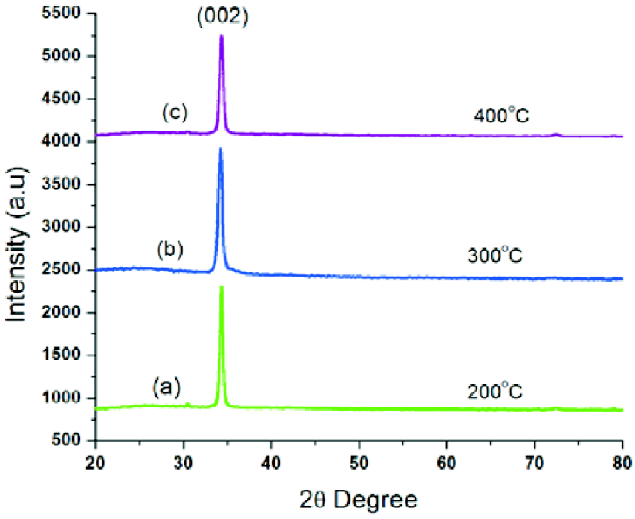

Fig. 5. XRD of ZnO:Al film on glass substrate with different substrate temperature (T_s).

Fig. 5 clearly shows that ZnO:Al thin film deposited at low T_s is of poor crystallinity and it improve when the T_s increased upto 400°C. As the T_s increases from 300°C to 400°C the intensity of the (002) peak decreases. At low T_s the sputtered atoms has less energy and the surface mobility is also low. Basically at T_s = 300°C, the substrate atoms have sufficient energy and the surface mobility is sufficient to make a stable position. And so it shows a stable c-axis orientation high intensity peak at (002) at 300°C. At 400°C the intensity of the peak (002) is decreases due to the breaking of Zn-O bonding, and re-evaporation of the deposited film started[20].

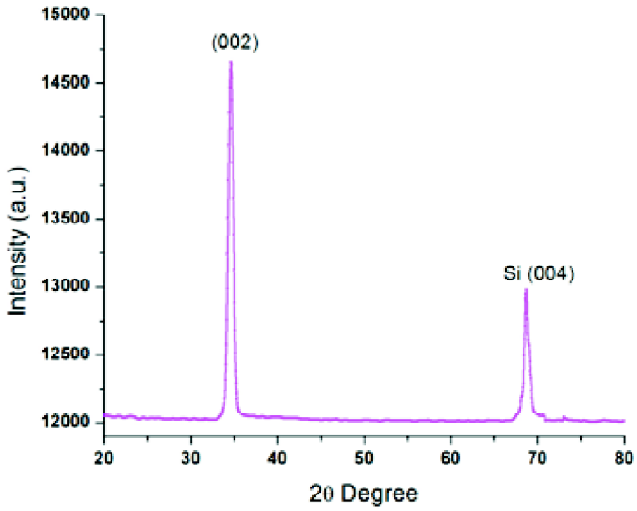

Fig. 6. XRD of ZnO:Al film on Si substrate.

The XRD spectrum of ZnO:Ga thin film (figure is not included) deposited at RT illuminating the hexagonal wurtzite structure. The ZnO:Ga sample prepared at RT shows diffraction peaks appearing at 2θ = 31.42°, 34.33° and 37.46° corresponding to (100), (002), and (101) planes, respectively.

It is clearly observed from the XRD blueprints that the peak (002) of the ZnO:Al on glass substrate is stronger and sharper than that on the PEN substrate. This indicates that the crystalline quality of the ZnO:Al film on glass substrate is much better than the PEN substrate and the thermal stability on the PEN substrate is poorer than the glass substrate. During bombardment of high energetic particles, the undesirable impurities escape from the PEN substrate and as a result the crystalline quality degrades of the ZnO:Al film for this PEN substrate.

The average crystallite sizes of the doped (Al, Ga) ZnO thin films deposited on different substrate temperatures have been calculated using the Scherrer's formula[21]:

$$D = \frac{0.0\lambda}{\beta \cos \theta} \quad (1)$$

The average crystallite sizes of the films grown at different substrate temperature are shown in Table 2. Dislocation densities have been calculated from this equation:

$$(\delta) = \frac{1}{D^2} \quad (2)$$

where $D = 0.9\lambda/\beta \cos\theta$ is the grain size in nm.

The average uniform strain e_{ZZ} in the lattice along the c-axis in the randomly oriented ZnO films deposited on different substrate temperatures (T_s) have been calculated from the lattice parameters using the following equation[22]:

$$e_{zz} = \frac{(C - C_0)}{C_0} \quad (3)$$

where C is the lattice parameter of ZnO film calculated from the (002) peak of the XRD pattern and C_0 is the lattice parameter for the ZnO bulk. The stress (σ) for hexagonal crystal in the plane of the film was calculated from the biaxial strain model[22]:

$$(\sigma) = \frac{[2C_{11} - (C_{11} - C_{12})C_{33}]}{C_{13}} e_{zz} \quad (4)$$

Here, $C_{11} = 2.1\times10^{11}$ N/m^2, $C_{33} = 2.1\times10^{11}$ N/m^2, $C_{12} = 1.2\times10^{11}$ N/m^2, $C_{13} = 1.05\times10^{11}$ N/m^2.

The estimated stress values, in the films grown at different T_s are shown in Table 2. From the Table 2, it is clear that negative sign indicates that the films are in a state of compressive stress. Basically there are two components are consists in total stress in the film. Among two components one is intrinsic stress that is introduced by impurities, defects and lattice distortions in the crystal, the other one is the extrinsic stress introduced by the lattice mismatch and thermal expansion coefficient mismatch between the film and substrate.

Is this study the film thickness are varies from 350 to 240 nm with substrate temperature. The present case of sputtering deposition, this intrinsic stress arises due to the bombardment of the energetic species. The extrinsic stress in the thin films normally relaxes if the thickness of the film is larger[23]. Thus the extrinsic stress are not present and the total estimated stress values seem to be dominantly intrinsic. The films deposited at lower temperature (room temperature) exhibit strong compressive stress. For high temperature deposited ZnO thin film, the strain quickly relaxed due to the high kinetic energy[24]. In the present case according to the growth conditions, the formation of Zn interstitials and the oxygen vacancies are expected. The presence of surface plasmon resonance (SPR) peak in the absorption spectra indicates the presence of extra Zn in the deposited films shown in Fig. 7. Thus, in the present case, the intrinsic stress in the deposited doped ZnO films seems to arise due to presence of Zn interstitials.

Fig. 7 shows the absorption spectra of ZnO:Al thin film deposited in different T_s. A broad peak at 262 nm and a smaller peak at 356 nm are observed. The peak around 356 nm corresponds to the ZnO excitation and the peak 262 nm corresponds to the surface plasmon resonance (SPR) peak. Lower temperature deposited films shows weak exciton peak of ZnO here as it is sharp and steeper with increases with the tem-

Table 2. Variation of crystalline size, lattice constant, grain size stress and strain of different substrate with different substrate temperature

Substrate type	Substrate temp. (T_s) (°C)	Lattice parameter (nm)	Grain size (nm)	Dislocation density (10^{15} lines/m^2)	Strain (e_{ZZ}) % ($\times10^{-3}$)	Stress (GPa)
ZnO:Al/Glass	27	0.5296	19.1	2.74	12.28	–5.526
	200	0.5265	21.4	2.18	10.49	–4.724
	300	0.5250	23.0	1.89	8.47	–3.812
	400	0.5206	24.2	1.70	4.04	–0.182
ZnO:Ga/Glass	27	0.5275	20.0	2.50	6.25	–0.124
	200	0.5263	22.0	2.01	4.80	–0.125
	300	0.5245	22.5	1.97	3.08	–0.135
	400	0.5241	23.0	1.89	2.82	–0.127
ZnO:Al/PEN	27	0.5201	25	1.61	2.27	–1.024
ZnO:Al/Si	27	0.5196	28	1.27	3.0	–0.135

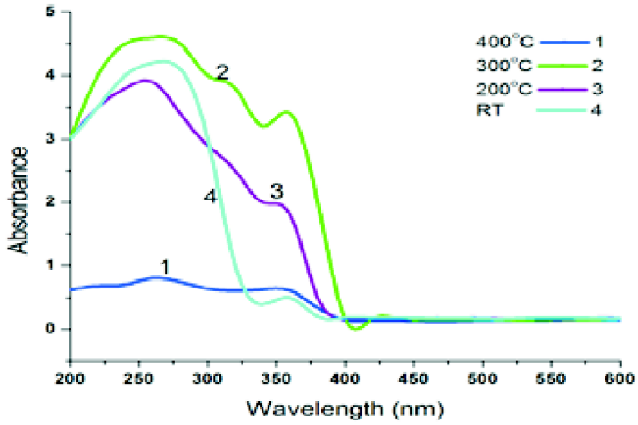

Fig. 7. Absorbance spectra of ZnO:Al thin film with different substrate temperature.

perature. High excitonic peak is the indication of good crystallinity of the film.

Band gap of the film deposited in different substrate was calculated from the relation $\alpha = (h\nu - E_g)^{1/2}$, where $h\nu$ is the photon energy and E_g is the transition energy gap. Fig. 8 shows the variations of bandgap of doped ZnO film with the substrate temperature. From this figure it is clearly observed that value of bandgap depends on the substrate temperature and it varies from 3.49 to 3.34 eV and 3.52 to 3.30 eV for ZnO:Al and ZnO:Ga respectively as the temperature increased from 27°C to 400°C. It was seen that the crystalline

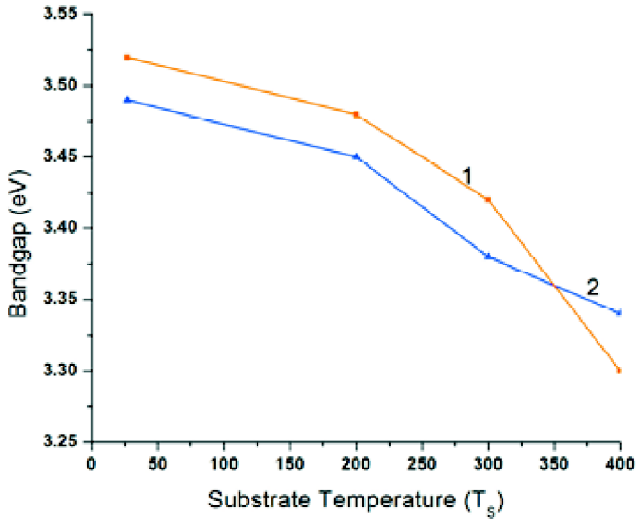

Fig. 8. Variation of band gap with different substrate temperature (T_s) of (1) ZnO:Al (red) and (2) ZnO:Ga (blue) films on glass substrate.

size of the doped (Al, Ga) ZnO thin film increases and there is relaxation of the intrinsic stress also with the increasing of substrate temperature. As the substrate temperature increases, the band gap decreases which attribute to the decrease in the stress. E_g of doped ZnO thin film on glass is wider than the PEN substrate. This is due to the higher carrier concentration of the doped ZnO films on glass according to the Burstein-Moss effect[25,26].

Haze is defined from the ratio of diffused transmission with that of total transmission. Haze value means more diffused light entre in to the cell as a result efficiency of the cell can be enhanced. Haze values of doped (Al, Ga) ZnO thin film on glass and PEN substrate are listed in Table 3. Proper formation of grain size (granular) of doped ZnO thin film can increase the light-scattering capability (i.e. the Haze) of the film. It helps to enhance the optical path as a result the light trapping ability is increased. Increasing light trapping ability means increasing the photocurrent of the solar cells[19]. In thin film solar cell ZnO thin film not only plays the role of TCO layer but also a light trapping structure. Crystal growth process depends on the kinetic and thermodynamic factors, leading to a different variation of surface morphologies[27–29].

Table 3. Haze factor of doped (Al, Ga) ZnO thin film on different substrate deposited at room temperature

Substrate type	%T	Bandgap (eV)	% Haze
Glass/ZnO:Al	90	3.49	40
Glass/ZnO:Ga	89	3.52	39
PEN/ZnO:Al	85	3.23	36

The detailed morphology and surface roughness of the RF magnetron sputtered doped (Al, Ga) ZnO thin films on different substrate were examined by AFM. Fig. 9(a) and 9(b) show the AFM of ZnO:Al on PEN and glass substrate respectively at room temperature. Fig. 9(c) for ZnO:Ga heat treated (at 300°C) on glass substrate. It is clearly observed from the figure that the grains grow uniformly with homogeneous distribution. The AFM images show a high-quality doped ZnO thin film with a smooth and crack-free surface. It is also observed that ZnO:Al films on glass and PEN substrate are all composed closely packed. RF magnetron is more preferred due to its reproducibility, high orientation and uniformity of thin films. Grain size the ZnO:Al films on PEN

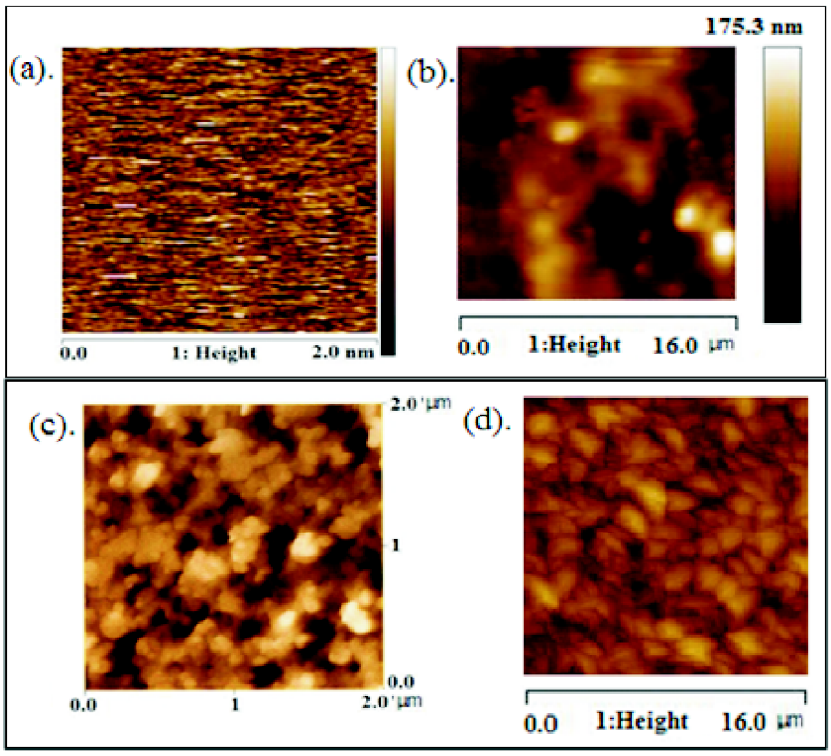

Fig. 9. AFM images of (a) ZnO:Al thin film on PEN substrate, (b) ZnO:Al on glass substrate, (c) ZnO:Ga on glass substrate and (d) ZnO:Al on Si substrate.

substrate (25 nm) is larger than that on glass substrate (24.2 nm). ZnO:Al thin film deposited on Si substrate [Fig. 9(d)] shows a stable structure with average grain size of 28 nm. For the application of ZnO thin films in silicon solar cells, the defects resulting from the ZnO grains must be as minimal as possible. When the ZnO grain size is high, the defects of ZnO thin films are minimized.

Conclusion

The influence of the substrate on the crystalline and oriented properties of ZnO thin films were grown by RF magnetron sputtering onto different substrates including glass, PEN and Si were investigated. Electrical, optical and structural properties of PEN substrate was measured after folding the film. All the films show high transmittance nearly 90% in the visible solar spectrum. Al, Ga doped ZnO thin films show nearly the same figure of merit value on glass and PEN substrate 1.08×10^{18} and 1.14×10^{18} respectively. AZO and GZO thin films show lowest resistivity of 4.9×10^{-4} Ω-cm and 4.6×10^{-4} Ω-cm on glass substrate. Room temperature deposited AZO film shows resistivity of 8.6×10^{-4} Ω-cm on PEN substrate.

Each films shows a preferred orientation along the (002) plane both at room temperature and high temperature. Film properties indirectly establish that doped (Al, Ga) ZnO thin films deposited on plastic substrate are crack free, mechanically stable and highly sticky with substrate surface. It was clearly observed from the result that the substrate nature has a strong factor influencing the properties of doped ZnO films. AZO thin film deposited on PEN substrate shows the commendable results for the application in the flexible display application. ZnO films grown on silicon substrate presented in this work have the potentiality to be a cost-effective alternative material for the substitution of the commercially available TCO materials[29] such as indium tin oxide (ITO) thin layer in heterojunction with intrinsic thin (HIT) layer solar cells.

Acknowledgement

The authors acknowledge the Department of Science and Technology, Govt. of India [DST/TM/SERI/2K10/67(G)] for

financial support, and also to Haldia Institute of Technology for infrastructure support.

References

1. K. L. Chopra, S. Major and K. D. Pandya, *Thin Solid Films*, 1983, **102**, 1.
2. M. D. Benoy, E. M. Mohammed, M. Suresh Babu, P. J. Binu and B. Pradeep, *Braz. J. Phys.*, 2009, **39**, 629.
3. J. Lee, D. Lee, D. Lim and K. Yang, *Thin Solid Films*, 2007, **515**, 6094.
4. S. M. Gates, *Mater. Res. Soc. Symp. Proc*., 1997, **467**, 843.
5. A. W. Macdonald, *J. Mater. Chem.*, 2004, **14**, 4.
6. H. L. Shen, H. Zhang, L.-Feng LU, F. Jiang and C. Yang, *Prog. Nat. Science: Mat. Int.*, 2010, **20**, 44.
7. R. Das H. S. Das, *J. Inst. Eng. (India)-D,* 2017, **98(1)**, 85.
8. R. Das and H. S. Das, *J. Inst. Eng. (India)-D,* 2017, **98(2)**, 203.
9. R. Das, H. S. Das, P. K. Nandi and S. Biring, *Appl. Phys. A*, 2018, **124**, 631.
10. S. Y. Lien, *Thin Solid Films,* 2010, **518**, S10.
11. M. Alvi, A. A. Ghamdi and M. Husain, *Physica B: Condensed Mat.*, 2017, **521**, 312.
12. D. K. Takci, E. S. Tuzemen, K. Kara, S. Yilmaz, R. Esen and O. Baglayan, *J. Mater. Sci. Mater. Electron.,* 2014, **25**, 2078.
13. M. Agarwal, P. Modi and R. O. Dusane, *J. Nano-Electron. Phys.,* 2013, **5(2)**, 02027.
14. X. Wang, X. T. Zeng, D. Huang and Q. Li, *J. Mater. Sci. Mater. Electron.,* 2012, **23(8)**, 1580.
15. B. Abdallah, A. K. Jazmati and R. Refaai, *Material Research*, 2017, **20(3)**, 607.
16. S. Hamrit, K. Djessas, N. Brihi, O. Briot, M. Moret and Z. Ben Ayadi, *J. Mater. Sci. Mater. Electron.,* 2016, **27**, 1730.
17. R. Ghosh, D. Basak and S. Fujihara, *J. Appl. Phys.*, 2004, **96**, 2689.
18. R. Kumar, N. Khare, V. Kumar and G. L. Bhalla, *App. Surface Science*, 2008, **254**, 6509.
19. J. Steinhauser, 'Low pressure chemical vapor deposited Zinc Oxide for thin film silicon solar cells', PhD Thesis, University de Neuchâtel, Switzerland, 2008.
20. Y. J. Kim, Y. T. Kim, H. K. Yang, J. C. Park, J. I. Han, Y. E. Lee and H. J. Kim, *J. Vac. Sci. Technol. A*, 1997, **15**, 1103.
21. B. D. Cullity and S. R. Stock, "Element of X-Ray diffraction", Prentice Hall, New Jersey, 2001, 170.
22. S. Maniv, W. D. Westwood and E. Colombini, *J. Vac. Sci. Technol*., 1982, **20**, 162.
23. T. B. Hur, Y. H. Hwang, H. K. Kim and I. J. Lee, *J. Appl. Phys.,* 2006, **99**, 064308.
24. R. Benger, K. Chang, P. Bhattachrya, J. Singh and K. K. Bajjaj, *Appl. Phys. Lett*., 1988, **53**, 684.
25. E. Burntein, *Phys. Rev.,* 1954, **93**, 632.
26. T. Moss, *Proc. Phys. Soc. B*, 1954, **67**, 775.
27. Y.-H. Hu, Y.-C. Chen, H.-J. Xu, H. Gao, W.-H. Jiang, F. Hu and Y.-X. Wang, *Engineering (Irvine, CA, U S)*, 2010, **2**, 973.
28. T. Shinagawa, K. Shibata, O. Shimomura, M. Chigane, R. Nomura and M. Izaki, *J. Mater. Chem. C,* 2014, **2**, 2908.
29. T. Mishima, M. Taguchi, H. Sakata and E. Maruyama, *Sol. Energ. Mat. Sol. Cells*, 2011, **95**, 18.